Surface Rainfall–Cold Cloud Fractional Coverage Relationship in TOGA COARE: A Function of Vertical Wind Shear

THOMAS R. SAXEN* AND STEVEN A. RUTLEDGE

Department of Atmospheric Science, Colorado State University, Fort Collins, Colorado

(Manuscript received 11 June 1998, in final form 23 February 1999)

ABSTRACT

Shipboard radar-derived rain rates and satellite-observed IR brightness temperatures have been used to examine the relationship between cold cloud fractional coverage for brightness temperatures <235 K and areally averaged surface rainfall during the Tropical Ocean–Global Atmosphere Coupled Ocean–Atmosphere Response Experiment (TOGA COARE). A nearly linear relationship was observed with a ratio of mean rain rate to fraction cold cloud coverage of approximately 1 mm h^{-1}. This is in contrast to the GOES precipitation index (GPI) methodology, which assumes a proportionality (GPI slope coefficient) of 3 mm h^{-1}.

It was also observed that when considering 5-day timescales, the relationship between the cold cloud fractional coverage and surface rainfall exhibited considerable variability. This variability was in phase with the interseasonal oscillations (ISOs). During the convectively active phase of the ISOs, the deep vertical wind shear (700–150 mb) was strong and the convective organization was dominated by squall line type systems. Hence, the cold cloud fractional coverage tended to be greater than the area of rainfall, a large fraction of which was stratiform in nature. The GPI slope coefficient was typically less than 1 mm h^{-1} during these periods. During the suppressed phase of the ISOs, tropospheric shear was much weaker and the convective organization consisted primarily of isolated convective cells. The cold cloud fractional coverage was typically about equal to the raining area, which was split nearly evenly between convective and stratiform precipitation. This resulted in a significant increase in the GPI slope coefficient, typically greater than 2 mm h^{-1} during these suppressed phases. It is also shown that during COARE, the variability in the GPI slope coefficient can to a large extent be explained by variations in tropospheric wind shear.

1. Introduction

The accurate measurement of rainfall over the tropical oceans has been, and remains, a difficult problem. Indeed more than two-thirds of the global precipitation falls in the Tropics between 30°N and 30°S (Simpson et al. 1988). The latent heat release associated with this rainfall is of fundamental importance for the development and maintenance of tropical circulations (Gill 1980). Accurate simulations of tropical circulation patterns in global general circulation models are presently hampered by incomplete knowledge of the spatial pattern and amount of tropical rainfall (latent heat release). It has also been observed that rainfall, especially that associated with convective systems, indirectly affects the surface energy budget by modifying the surface fluxes of heat, moisture, and momentum (Johnson and Nicholls 1983; Young et al. 1995; Jabouille et al. 1996; Saxen and Rutledge 1998). In addition, rainfall is an extremely important variable from an oceanographic standpoint. When rainfall occurs over the tropical oceans, heat fluxes (cold rain falling on warm surface water; Flament and Sawyer 1995; Gosnell et al. 1995) and buoyancy fluxes (freshwater falling on saltwater; Price 1979; Tomczak 1995) provide for large dynamic and thermodynamic responses in the upper ocean (Miller 1976; Lukas and Lindstrom 1991; Lukas 1990). This atmosphere–ocean coupling is closely linked to climate variations such as El Niño–Southern Oscillation (ENSO; Philander 1990).

In the tropical western Pacific, these factors are paramount since this is one of the most convectively active regions of the world, with areally averaged rainfall in excess of 3 m $year^{-1}$ (extrema of over 5 m $year^{-1}$) (Taylor 1973). This was one of the primary factors behind conducting the Tropical Ocean–Global Atmosphere Coupled Ocean–Atmosphere Response Experiment (TOGA COARE) in the western Pacific warm pool. Webster and Lukas (1992) provided a comprehensive overview of TOGA COARE. One of the scientific objectives of COARE was to determine the distribution and variability of precipitation in the western

* Current affiliation: National Center for Atmospheric Research, Boulder, Colorado.

Corresponding author address: Thomas R. Saxen, National Center for Atmospheric Research, Boulder, CO 80307.
E-mail: saxen@ucar.edu

Pacific warm pool with the end result being improved models of the global general circulation, which will further our understanding of climate variations (Webster and Lukas 1992).

During COARE, rainfall was observed with numerous platforms ranging from various types of rain gauges, to Doppler radars on ships and aircraft, to satellites. Rain gauges provide rainfall information with excellent temporal resolution, but since they provide only a small number of point measurements, their use in global rainfall estimation is limited to a few areas where there is adequate spatial sampling. Quantitative radar observations offer improved spatial coverage, but these observations will never be routine over the open ocean. Therefore, satellite observations are best suited for global rainfall estimation since they provide excellent spatial coverage on a nearly continuous basis with ample temporal resolution (typically 2–24+ observations per day). However, some of the satellite-based rainfall estimation techniques are empirical rather than physically based methods, and therefore it is very important to investigate these algorithms with more direct rainfall observations when the opportunity arises, especially over the open ocean where direct observations are scarce. TOGA COARE provided such an opportunity for the tropical western Pacific warm pool region.

Arkin and Ardanuy (1989) provided a review of several satellite-based rainfall estimation methodologies. One widely employed method of rainfall estimation is the Geostationary Operational Environmental Satellite (GOES) precipitation index (GPI; Arkin and Meisner 1987). This method, which was developed using IR and radar data collected during GATE [GARP (Global Atmospheric Research Program) Atlantic Tropical Experiment], was based on the work of Arkin (1979) and Richards and Arkin (1981), which indicated a nearly linear relationship between areally averaged surface rainfall and the fractional coverage below a specified IR brightness temperature. Arkin (1979) examined this relationship for the GATE B-array (a hexagonal area extending from 22.25° to 24.75°W and from 7° to 10°N) using 6-h average values of radar-derived surface rainfall and various cloud-top temperature thresholds between 205 and 280 K. The highest correlations were observed for the 235 K threshold. Richards and Arkin (1981) explored the effects of averaging over various spatial and temporal scales. The spatial scales in their study ranged from 0.5° to 2.5° lat and the temporal scales ranged from 1 to 24 h. Richards and Arkin reported that the correlations between surface rainfall and cold cloud fractional coverage generally improved with larger spatial scales and longer temporal scales. The GPI methodology developed by Arkin and Meisner (1987) uses monthly averaged values of fractional coverage below the 235 K brightness temperature threshold for 2.5° by 2.5° regions. The relation devised by Arkin and Meisner employed a regression coefficient (hereafter referred to as the GPI slope coefficient) of 3 mm h^{-1} and was given by

$$\mathrm{GPI} = 3 \cdot \mathrm{FC235} \cdot t, \tag{1}$$

where GPI is in mm, FC235 is the fractional cold cloud coverage below the 235 K IR brightness temperature threshold (between 0 and 1), and t is the time (in hours) for which FC235 was computed. Upon rearranging (1), it can be immediately seen that the GPI slope coefficient is simply the ratio of the areal rain rate (GPI/t) to FC235. Equation (1) was used by Arkin and Meisner (1987) to produce seasonal (3 month) mean rainfall estimates for the 3-yr period from December 1981 to November 1984. Their results, including the seasonal cycle, showed no systematic biases and compared very well with similar published climatologies for the tropical oceans. Therefore, they concluded that this method can be used to provide useful rainfall estimates for time periods from months to years over the tropical oceans. Indeed, GPI is currently an integral component of a number of global rainfall estimation algorithms (Xie and Arkin 1996, 1997). For this reason, we chose to focus our attention on the relationship between surface rainfall and the cold cloud fractional coverage below the 235 K brightness temperature threshold. These algorithms are used to produce global monthly rainfall estimates with 2.5° horizontal resolution. However, increased temporal and spatial resolution is desired, requiring improvements in the individual components of the algorithms (Xie and Arkin 1997).

Not only is the western Pacific warm pool an important region for studying the relationship between cold cloud fractional coverage and rainfall due to the large amount of rainfall in this region, but this region is also important since the 40–50-day interseasonal oscillation (ISO) is known to modulate both precipitation (Hartmann and Gross 1988) and convective cloudiness (Lau and Chan 1985; Nakazawa 1988; Chen et al. 1996) in the western Pacific. Chen et al. (1996) reported that ISOs dominated the convective variability in the Indian–Pacific warm pool region during COARE, being marked by extensive eastward propagating cold cloud clusters. During the most convectively active periods, the cloud clusters became so large and numerous that they could no longer be individually identified. Rickenbach and Rutledge (1998) reported that Mesoscale Convective System– (MCS-) scale linear systems (i.e., linearly organized systems with a spatial scale greater than 100 km) were much more common during the westerly wind phases of the ISOs. Furthermore, these systems produced the majority of the rainfall observed by radar during COARE. Therefore, one might also suspect that ISOs also affect the relationship between rainfall and fractional coverage of cold cloud as used in a GPI relationship. Arkin and Xie (1994) found systematic variations in the areal surface rainfall–cold cloud fractional coverage over Japan during the First Global Precipitation Climatology Project (GPCP) Algorithm Intercom-

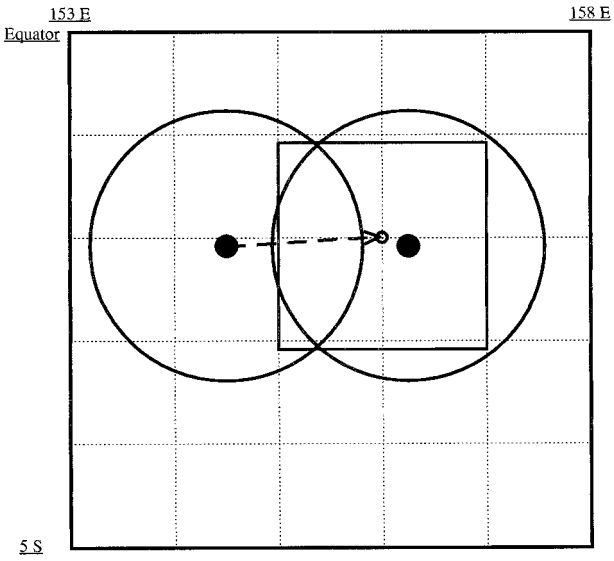

FIG. 1. Nominal deployment positions with 145-km range rings for the R/V *Xiang Yang Hong #5* (left circle) and the R/V *John V. Vickers* (right circle). Also shown is the 2° × 2° grid box (centered at 2.083°S, 156°E) for which the mean rain rates and fractional coverage below the 235 K IR brightness temperature threshold were calculated. The small open circle at 2°S, 156°E shows the nominal position when only one ship was present.

parison Project (AIP-1). They correlated these variations with surface pressure observations, finding significant variations during ''low,'' ''prelow,'' and ''postlow'' periods.

The primary objective then of this work is to explore the surface rainfall–cold cloud fractional coverage relationship during COARE. The variability in this relationship will be explored within the context of environmental vertical wind shear as it relates to anvil growth relative to system motion and controlling the organization of convection. It will be shown that the deviations in this relationship are in phase with the ISOs, with the majority of the variability explained by variations in deep vertical wind shear (700–150 mb). An explanation for this response, based on the modulation of convective organization, also will be presented.

2. Data

The TOGA COARE intensive observation period (IOP), which took place in the tropical western Pacific from November 1992 through February 1993, provided a prime opportunity to explore the relationship between cold cloud fractional coverage and surface rainfall in this region. During COARE, two research vessels had C-band Doppler radars on board (the TOGA radar on the R/V *Xiang Yang Hong #5* and the Massachusetts Institute of Technology (MIT) radar on the R/V *John V. Vickers*) that provided radar reflectivity data, which, after appropriate processing, were used to provide an estimate of the areal surface rainfall. The rain-rate data

TABLE 1. Number of individual days and 5-day periods for each IOP that were used in the current study. The time ranges for the three IOPs are based on the shipboard radar deployment schedule (Short et al. 1997).

IOP No.	No. of days (No. missing)	No. of 5-day periods
IOP 1	37	7
(5 Nov–11 Dec 1992)	(1)	
IOP 2	36	7
(14 Dec 1992–18 Jan 1993)	(2)	
IOP 3	32	6
(23 Jan–23 Feb 1993)	(4)	
Total	105	20
	(7)	

used in this study were provided by the National Aeronautics and Space Administration (NASA) Tropical Rainfall Measuring Mission (TRMM) office and had a temporal resolution of 10 min and a spatial resolution of 2 km. The reflectivity fields were separated into convective and stratiform rain areas following the technique of Steiner et al. (1995) and separate *Z–R* relations (deduced by Tokay and Short 1996) were applied to obtain the rain rates. An overview of this dataset including a discussion on the data processing procedures is provided by Short et al. (1997).

Hourly IR (10.5–12.5 μm) data (spatial resolution of 11 km) from the Japanese Geostationary Meteorological Satellite (*GMS-4*) were used to compute FC235. The FC235 and the mean rain rates were calculated for a 2° by 2° grid box centered at 2.083°S, 156°E. This grid box along with the nominal radar coverage area is depicted in Fig. 1.

The rain rate and satellite data described above were used to first compute daily averages of rain rate, fractional rain area (including convective and stratiform components), and FC235. If more than 25% of the data were missing or bad that individual data point was not included. Then if at least 75% of the rain rate and satellite data were present (in a temporal sense), a daily average was computed. These daily averaged values were then matched in pairs to produce the 5-day averages using the same 75% minimum criteria. Also, consecutive days were required. The data were separated into consecutive 5-day sections and if only four consecutive days were left in a particular section it was included since it met the 75% minimum criteria. Table 1 summarizes the number of individual days and 5-day periods for the three COARE IOPs that were included in this analysis.

Vertical wind shear was calculated using daily averaged 2.5° gridded National Centers for Environmental Prediction–National Center for Atmospheric Research (NCEP–NCAR) reanalysis zonal and meridional wind data (Kalnay et al. 1996). The shear was calculated for the 2.5° grid box that encompassed 2.083°S, 156°E. Shears were calculated for various depth intervals with the largest correlation between vertical wind shear and

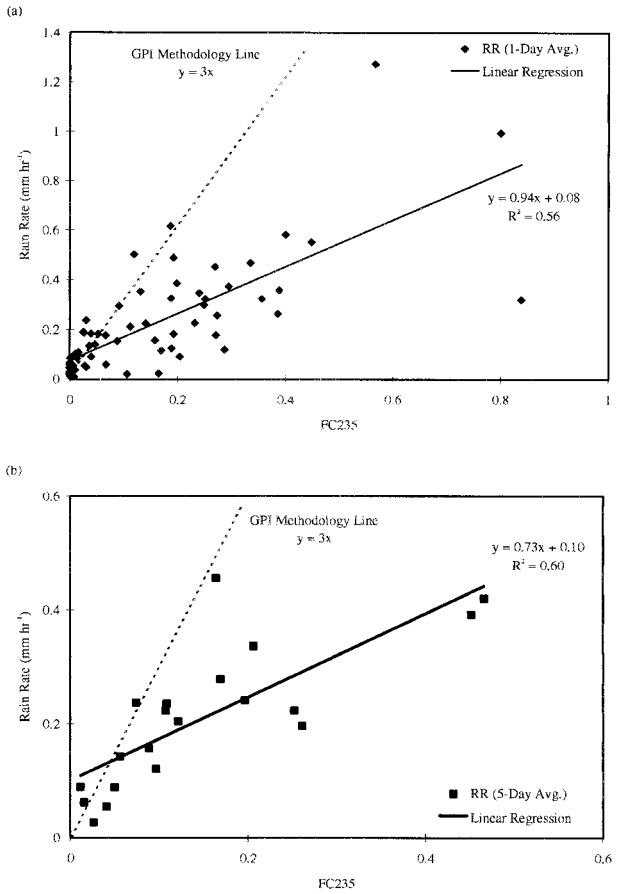

FIG. 2. The radar-derived areally averaged surface rain rate as a function of FC235 for the 2° × 2° grid box depicted in Fig. 1. The (a) daily and (b) 5-day averaged values are shown. Results of the linear regression analysis are plotted as a solid line along with the corresponding equation and correlation coefficient squared. The dashed line depicts what would be expected based on the GPI methodology.

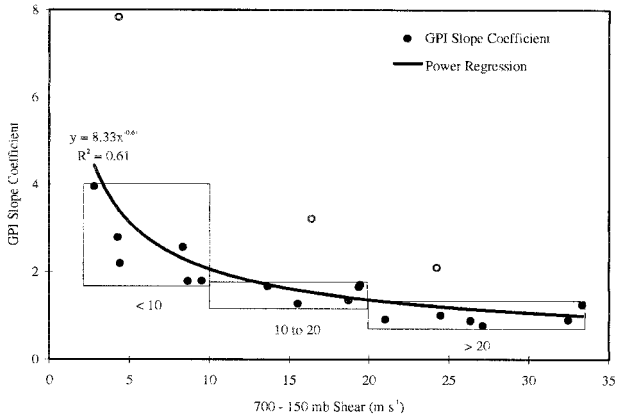

FIG. 3. The 5-day GPI slope coefficient as a function of the 700–150-mb vertical wind shear. The results of a power regression analysis are plotted as a solid line along with the corresponding equation and correlation coefficient squared. The boxes enclose all points (solid), which fall within one standard deviation from the mean for three shear intervals (<10 m s^{-1}, 10 to 20 m s^{-1}, and >20 m s^{-1}). Points greater than one standard deviation from the mean are shown as open circles.

variations in GPI slope coefficient being observed for the 700–150-mb interval. Therefore, only the 700–150-mb vertical wind shear values will be utilized and presented in this study.

The above-described data were used to produce 5-day averages. The use of 5-day averages was adopted since this eliminated much of the scatter evident in the daily data and since current efforts include producing 5-day rainfall estimates (P. Arkin 1997, personal communication). The use of 5-day mean values also helps to illustrate the variability in the GPI slope coefficient during COARE and allows the phasing with the ISOs to be easily recognized.

3. Results

a. Surface rainfall–cold cloud fractional coverage relationship

Shipboard radar observations and IR satellite observations were used in GATE to show that there was a nearly linear relationship between cold cloud fractional coverage and areally averaged surface rainfall (Arkin 1979; Richards and Arkin 1981). Those studies demonstrated that this relationship was fairly insensitive to variations in the temporal and spatial averaging scales, provided that the scales were sufficiently large (temporal scales > 6 h and spatial scales > approximately 1.5°). However, the correlations generally increased with increasing averaging scales. A similar analysis was performed using data collected during TOGA COARE and the results for both daily and 5-day averages are shown in Fig. 2. During COARE there was also a nearly linear relationship between FC235 and the surface rain rate, but there was considerably more variability compared to GATE, even in the 5-day averages (i.e., the correlations were lower). The slope was also significantly smaller than that deduced in GATE, less than 1 mm h^{-1} compared to 3 mm h^{-1}. A similar trend was observed by Morrissey and Greene (1993),who employed Pacific atoll rain gauge data to verify the GPI methodology and suggested a slope correction factor of about 0.67 (or a value of about 2 mm h^{-1} rather than 3 mm h^{-1}) for the Pacific region. The intercepts in Fig. 2 (about 0.1 mm h^{-1}), which is not included in the GPI methodology, are similar to those observed in GATE (about 0.1–0.2 mm h^{-1}; Richards and Arkin 1981) and also to those suggested by Morrissey and Greene (1993) (approximately 0.1 mm h^{-1}).

b. GPI coefficient variations with deep vertical shear

The GPI slope coefficient during COARE, plotted as a function of 700–150 mb shear in Fig. 3, was highly variable. It is clear from Fig. 3 that as the deep shear increases, the GPI coefficient decreases and becomes

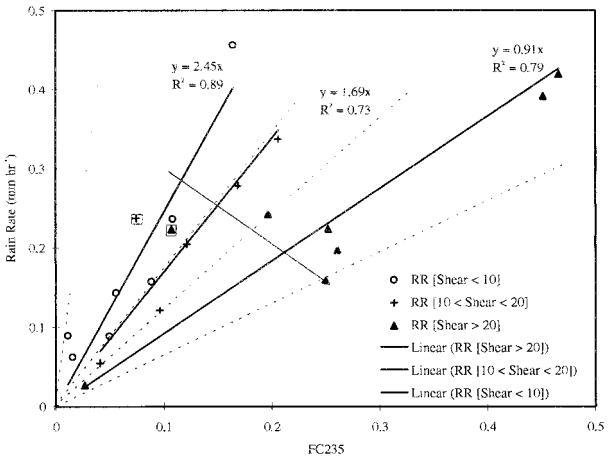

FIG. 4. Same as Fig. 2b but the points are divided into three 700–150-mb vertical wind shear intervals (<10 m s^{-1}, 10 to 20 m s^{-1}, and >20 m s^{-1}). The results of linear regression analyses for these three intervals are plotted as solid lines along with the corresponding equations and correlation coefficients squared. Dashed lines depict the observed ranges for the three intervals, not including two outliers, which are shown enclosed in squares. The arrow indicates the direction of increasing shear.

less variable (i.e., levels out at a value slightly less than 1 mm h^{-1}). The 5-day FC235–surface rain-rate relationship is reproduced in Fig. 4; however, the relationship is broken down into three deep shear intervals (<10 m s^{-1}, 10 to 20 m s^{-1}, and >20 m s^{-1}). These intervals were chosen since they resulted in approximately equal numbers of 5-day periods in each interval (6 or 7). Here again it is evident that as the shear increases, the GPI slope coefficient systematically decreases. This suggests that a correction factor based on the magnitude of the deep shear may be possible for the western Pacific warm pool region.

The variations in the GPI slope coefficient were observed to be in phase with the ISOs that were observed during COARE. Figure 5 depicts variations in the GPI slope coefficient along with the 850-mb zonal wind and 700–150-mb vertical wind shear. The three ISOs that were observed during COARE are indicated by a solid line near the bottom of Fig. 5 (Lin and Johnson 1996). It is evident that when the wind shear was strong and the 850-mb zonal wind was strong and westerly, the GPI slope coefficient had a value near 1 mm h^{-1}. When the wind shear was weak and the 850-mb zonal wind was weak and/or easterly, the GPI slope coefficient was significantly larger. Because of this phasing with the ISOs, the effects that ISOs have on the cold cloud fractional coverage–surface rainfall relationship were examined in more detail.

Since ISOs significantly controlled the convective activity in COARE (Chen et al. 1996; Rickenbach and Rutledge 1998), variations in the organization of convection with deep shear were explored. The convective classification procedure described in Rickenbach and Rutledge (1998) was adopted to diagnose the dominant modes of convective organization for the three deep shear intervals discussed above. The systems were classified based on spatial scale and horizontal morphology of the contiguous radar echoes. Systems whose radar echoes had spatial scales larger than 100 km were classified as MCS-scale systems whereas those with smaller spatial scales were classified as sub-MCS-scale systems.

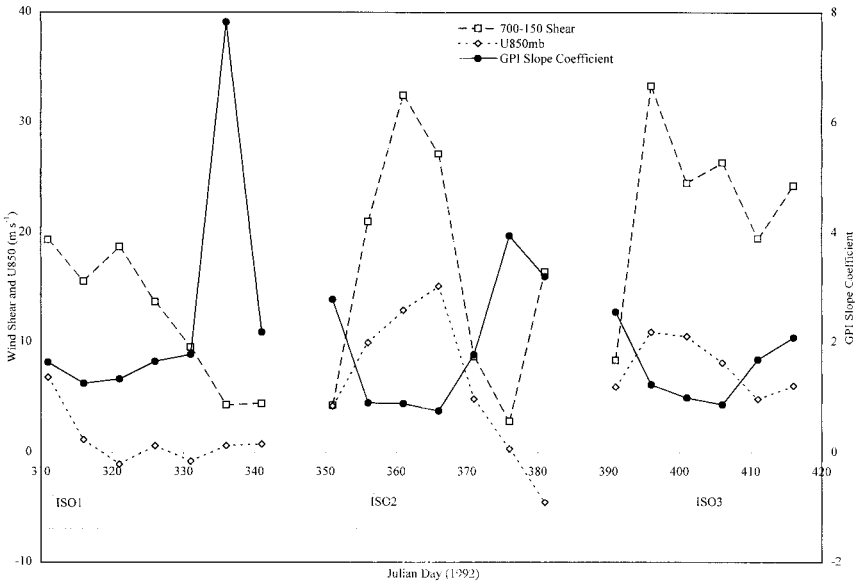

FIG. 5. Time series of the GPI slope coefficient, 850-mb zonal wind (U850mb), and 700–150 mb vertical wind shear. Five-day means values are shown. Near the bottom of the figure, the three ISO periods observed during COARE are indicated by the solid line [following Lin and Johnson (1996)].

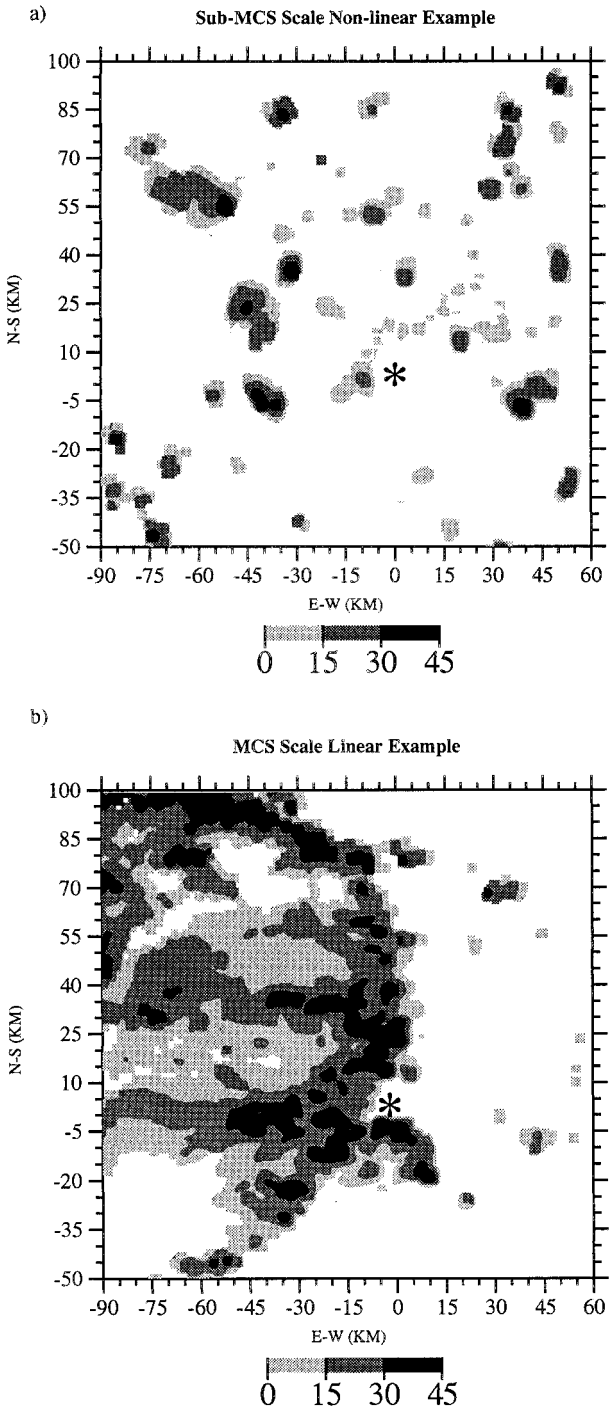

FIG. 6. Example of (a) sub-MCS-scale nonlinear and (b) MCS-scale linear types of convective organization (following Rickenbach and Rutledge 1998). Reflectivity values are in dBZ.

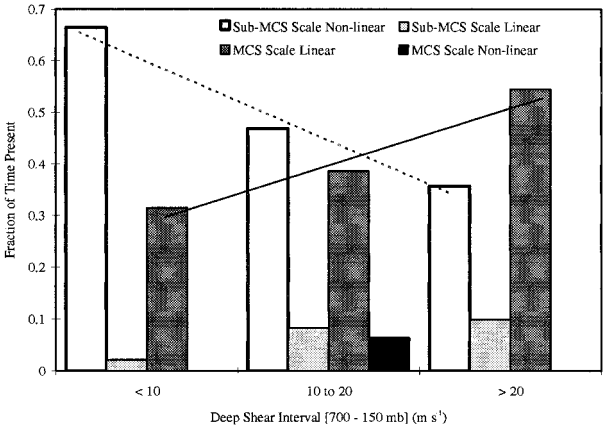

FIG. 7. The modes of convective organization (presented as fraction of time present) for three 700–150-mb vertical wind shear intervals. The convective organization classification procedures are from Rickenbach and Rutledge (1998).

Systems were also classified as being linearly organized if the radar echoes exhibited linear organization during their life cycle and nonlinear if no linear organization was observed. The two dominant modes were sub-MCS-scale nonlinear and MCS-scale linear systems, being present about 48% and 43% of the time, respectively (Rickenbach and Rutledge 1998). Examples of these two modes of convective organization are provided in Fig. 6. Figure 7 shows that when the deep shear was weak (<10 m s^{-1}), the primary mode of convective organization was sub-MCS-scale nonlinear systems, present about 65% of the time. As the deep shear increased, the primary mode of convective organization shifted to MCS-scale linear systems, which were the dominant convective mode 55% of the time when the deep shear was greater than 20 m s^{-1}. How convection is organized can affect the cold cloud fractional coverage–surface rainfall relationship in two ways: through the area raining–cold cloud fractional coverage relationship and the magnitude of rain rates within the raining area (i.e., relative amounts of convective and stratiform rain areas). These two considerations will be explored in the following sections.

c. Rain area–cold cloud fractional coverage variations

Figure 8 depicts how the ratio of the raining area to FC235 varied with the 700–150-mb shear. When the deep shear was greater than 10 m s^{-1}, the FC235 was typically slightly larger than the raining area, whereas when the deep shear was less than 10 m s^{-1} there was an increased tendency for the raining area to be larger than the FC235 (there is a tendency for the ratio to decrease with increasing shear). This behavior is consistent with the trends in the convective organization shown in Fig. 7. Rickenbach and Rutledge (1998) reported that sub-MCS-scale nonlinear systems, which by definition are small in size, tended to have rather shallow radar reflectivity features, the vast majority of which were less than 8 km deep. The GPI methodology was not designed to account for rainfall from such features (Arkin and Meisner 1987). However, these types of sys-

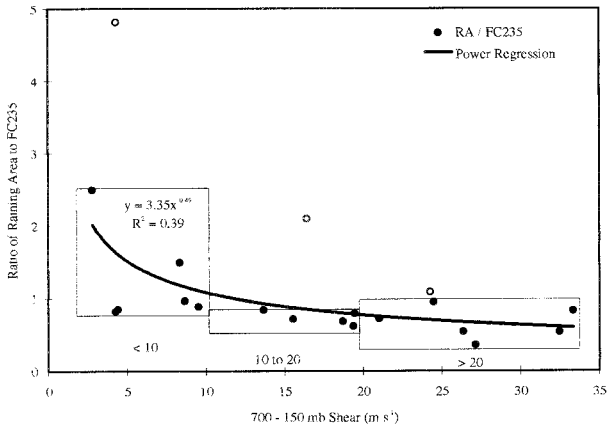

FIG. 8. Same as Fig. 3 except for the ratio of the raining area (RA) to FC235.

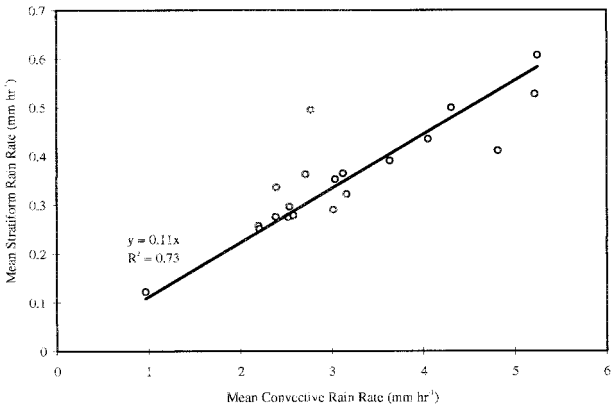

FIG. 9. The mean stratiform rain rate within the stratiform rain area as a function of the mean convective rain rate within the convective rain area. The result of a linear regression analysis is plotted as solid lines along with the corresponding equation and correlation coefficient squared.

tems produced a nonnegligible fraction (13%) of the rainfall observed by the MIT radar during COARE (Rickenbach and Rutledge 1998). MCS-scale linear systems (i.e., squall line–like systems) tended to contain much deeper convective features, a large fraction of which were deeper than 10 km (Rickenbach and Rutledge 1998). The deep nature of these systems and their associated flow features also aid in the production of horizontally extensive anvil clouds (Zipser et al. 1981; Gamache and Houze 1982). These anvils were frequently observed to extend well beyond the area of rainfall at the surface (Houze 1977; Zipser 1977) and existed well after the rainfall ceased (Zipser et al. 1981).

d. Rain type variations

Since the rain rates were separated into convective and stratiform components (Short et al. 1997), the fractional stratiform and convective rain areas for the 2° by 2° analysis region were calculated so that their relative importance could be addressed. The mean rain rate in the convective rain areas was about 10 times larger than that in the stratiform rain areas (Fig. 9). Therefore, when the stratiform rain area is significantly larger than the convective rain area, the areal rain rate will be smaller when compared to a similarly sized raining area in which the stratiform and convective rain areas are about equal. Figure 10 depicts how the ratio of stratiform rain area to convective rain area varied with the 700–150-mb shear. As the deep shear increased, there was a general trend of increasing stratiform rain area compared to convective rain area. Therefore, a larger fraction of the raining area consists of light (stratiform) rainfall, resulting in a lower mean rain rate per unit raining area, which would yield a lower GPI slope coefficient. This increase in stratiform precipitation with tropospheric shear is also consistent with the trends in the convective organization shown in Fig. 7. Rickenbach and Rutledge (1998) reported that for MCS-scale linear systems, a significant stratiform component was typically present, whereas for sub-MCS-scale nonlinear systems, stratiform precipitation was not present. Numerous previous studies have reported significant stratiform precipitation with tropical squall line–like systems (e.g., Houze 1977; Zipser 1977; Gamache and Houze 1983; Houze and Rappaport 1984).

4. Conclusions

The cold cloud fractional coverage–surface rainfall relationship during TOGA COARE has been examined in this study. It was noted that the areally averaged surface rainfall and the cold cloud fractional coverage are related in a nearly linear fashion similar to what was observed during GATE, but overall, the GPI slope coefficient in COARE was much closer to 1 mm h^{-1} than to 3 mm h^{-1} as had been deduced during GATE. A similar trend (i.e., a GPI slope coefficient less than 3 mm h^{-1}) was suggested by Morrissey and Greene (1993) in their study, which made use of gauge data from Pa-

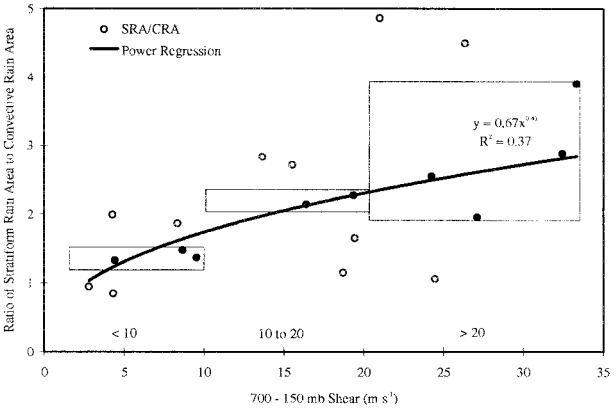

FIG. 10. Same as Fig. 3 except for the ratio of the stratiform rain area (SRA) to the convective rain area (CRA).

cific atolls. Morrissey and Greene attributed this behavior to the nature of convective systems in the Pacific compared to the Atlantic. They hypothesized that the convective activity in the Pacific is much deeper and hence produces much larger cold cloud areas. LeMone et al. (1998) also reported that the convective systems observed during COARE were deeper than those observed during GATE due to the convective equilibrium level being much higher than in the GATE study area. The current study relates the shorter timescale (5-day) variability in the areal rain rate–cold cloud fractional coverage relationship to the phase of the ISO, which significantly modulates the organization of convection in this region. DeMott and Rutledge (1998) presented observations from COARE that the depths of the convective systems were modulated by the ISO.

On short timescales (i.e., 5 days) the GPI slope coefficient exhibited considerable variability, which was in phase with the ISOs observed during COARE. During the strong westerly phase of the two most prominent ISOs, the deep (700–150 mb) vertical wind shear was very strong (>20 m s^{-1}) and the majority of the convective systems were classified as MCS-scale linear systems. The majority of these systems were faster moving and shorter lived than those observed during GATE (LeMone et al. 1998). The FC235 was typically somewhat larger than the raining area and the stratiform rain areas (i.e., lighter rain areas) were significantly larger than the convective rain areas (i.e., heavier rain areas), typically larger by a factor of 3–4. This predominance of light rainfall in conjunction with the FC235 being larger than the raining area resulted in a small GPI slope coefficient (approximately 1 mm h^{-1}, ± 0.25 mm h^{-1}).

In contrast, during the weak wind phases, the deep vertical wind shear was much weaker (<10 m s^{-1}) and the GPI slope coefficient was significantly higher, typically greater than about 2 mm h^{-1}. The convective organization was dominated by sub-MCS-scale nonlinear systems and the raining area was approximately equal to or larger than the FC235. The stratiform rain areas were much more comparable in size to the convective rain areas, being only about 1.4 times larger in size on average. Since the majority of the rainfall and cloudiness were observed during the westerly wind phase, these points receive more weight in the regression analysis than the limited rainfall/cloudiness points and thus, the overall GPI slope coefficient was close to 1 mm h^{-1}.

This study has shown that if GPI-like methods are to be employed to estimate rainfall on 5-day timescales in the western Pacific warm pool, there may be significant biases present that are linked to the phase of ISOs, which are known to propagate through and intensify over this region. These would appear as high biases during the strong westerly wind phase (i.e., convectively active phase) and low biases during the weak wind phase (i.e., suppressed phase). Morrissey and Greene (1993) also observed similar biases in the western Pacific, but a connection to ISOs was not shown. Arkin and Xie (1994) reported similar variations during AIP/1 over Japan, but they correlated the variations with changes in surface pressure. Arkin and Xie stressed that if the circumstances that lead to these variations can be identified, significantly improved rainfall estimates could be possible. During COARE, a large fraction (approximately 60%) of the variability in the GPI slope coefficient was accounted for by variations in deep vertical shear, which was primarily modulated by ISOs. This suggests that a correction factor for the GPI methodology, which is related to deep vertical wind shear may be possible for the western Pacific warm pool region.

Acknowledgments. We received valuable comments and suggestions during the early stages of this work from Dr. Phil Arkin. Dr. Edward Zipser and two anonymous reviewers are acknowledged for the comments they supplied, which led to improvements in this manuscript. The following provided data that were vital to this study: NASA TRMM Office (radar-derived rainrate data), NOAA Climate Diagnostic Center (NCEP reanalysis wind data), and Dr. T. Nakazawa, MRI, Japan (*GMS-4* IR satellite data). This research was supported under TOGA COARE Grant NA37RJ0202 from the National Oceanic and Atmospheric Administration Office of Global Programs.

REFERENCES

Arkin, P. A., 1979: The relationship between fractional coverage of high cloud and rainfall accumulations during GATE over the B-scale array. *Mon. Wea. Rev.,* **107,** 1382–1387.

——, and B. N. Meisner, 1987: The relationship between large-scale convective rainfall and cold cloud over the western hemisphere during 1982–84. *Mon. Wea. Rev.,* **115,** 51–74.

——, and P. E. Ardanuy, 1989: Estimating climatic-scale precipitation from space: A review. *J. Climate,* **2,** 1229–1238.

——, and P. Xie, 1994: The Global Precipitation Climatology Project: First Algorithm Intercomparison Project. *Bull. Amer. Meteor. Soc.,* **75,** 401–419.

Chen, S. S., R. A. Houze Jr., and B. E. Mapes, 1996: Multiscale variability of deep convection in relation to large-scale circulation in TOGA COARE. *J. Atmos. Sci.,* **53,** 1380–1409.

DeMott, C. A., and S. A. Rutledge, 1998: The vertical structure of TOGA COARE convection. Part I: Radar echo distributions. *J. Atmos. Sci.,* **55,** 2730–2747.

Flament, P., and M. Sawyer, 1995: Observations of the effect of rain temperature on the surface heat flux in the intertropical convergence zone. *J. Phys. Oceanogr.,* **25,** 413–419.

Gamache, J. F., and R. A. Houze Jr., 1982: Mesoscale air motions associated with a tropical squall line. *Mon. Wea. Rev.,* **110,** 118–135.

Gill, A. E., 1980: Some simple solutions for heat-induced tropical circulation. *Quart. J. Roy. Meteor. Soc.,* **106,** 447–462.

Gosnell, R., C. W. Fairall, and P. J. Webster, 1995: On the heat budget of the equatorial west Pacific surface mixed layer. *J. Geophys. Res.,* **100,** 18 437–18 442.

Hartmann, D. L., and J. R. Gross, 1988: Seasonal variability of the 40–50 day oscillation in wind and rainfall in the Tropics. *J. Atmos. Sci.,* **45,** 2680–2702.

Houze, R. A., Jr., 1977: Structure and dynamics of a tropical squall-line system. *Mon. Wea. Rev.,* **105,** 1540–1567.

——, and E. N. Rappaport, 1984: Air motions and precipitation struc-

ture of an early summer squall line over the eastern tropical Atlantic. *J. Atmos. Sci.,* **41,** 553–574.

Jabouille, P., J. L. Redelsperger, and J. P. Lafore, 1996: Modification of surface fluxes by atmospheric convection in the TOGA COARE region. *Mon. Wea. Rev.,* **124,** 816–837.

Johnson, R. H., and M. E. Nicholls, 1983: A composite analysis of the boundary layer accompanying a tropical squall line. *Mon. Wea. Rev.,* **111,** 308–319.

Kalnay, E., and Coauthors, 1996: The NCEP/NCAR 40-Year Reanalysis Project. *Bull. Amer. Meteor. Soc.,* **77,** 437–472.

Lau, K. M., and P. H. Chan, 1985: Aspects of the 40–50 day oscillation during the northern winter as inferred from outgoing longwave radiation. *Mon. Wea. Rev.,* **113,** 1889–1909.

LeMone, M. A., E. J. Zipser, and S. B. Trier, 1998: The role of environmental shear and thermodynamic conditions in determining the structure and evolution of mesoscale convective systems during TOGA COARE. *J. Atmos. Sci.,* **55,** 3493–3518.

Lin, X., and R. H. Johnson, 1996: Kinematic and thermodynamic characteristics of the flow over the western Pacific warm pool during TOGA COARE. *J. Atmos. Sci.,* **53,** 695–715.

Lukas, R., 1990: The role of salinity in the dynamics and thermodynamics of the western Pacific warm pool. *Proc. Int. TOGA Scientific Conf.,* Honolulu, HI, World Meteorological Association, 73–113.

——, and E. Lindstrom, 1991: The mixed layer of the western Pacific Ocean. *J. Geophys. Res.,* **96,** 3343–3357.

Miller, J. R., 1976: The salinity effect in a mixed layer ocean model. *J. Phys. Oceanogr.,* **6,** 29–35.

Morrissey, M. L., and J. S. Greene, 1993: Comparison of two satellite-based rainfall algorithms using Pacific atoll raingage data. *J. Appl. Meteor.,* **32,** 411–425.

Nakazawa, T., 1988: Tropical super clusters within interseasonal variation over the western Pacific. *J. Meteor. Soc. Japan,* **66,** 823–839.

Philander, S. G., 1990: *El Niño, La Niña, and the Southern Oscillation.* Academic Press, 293 pp.

Price, J. F., 1979: Observations of a rain-formed mixed layer. *J. Phys. Oceanogr.,* **9,** 643–649.

Richards, F., and P. A. Arkin, 1981: On the relationship between satellite-observed cloud cover and precipitation. *Mon. Wea. Rev.,* **109,** 1081–1093.

Rickenbach, T. M., and S. A. Rutledge, 1998: Convection in TOGA COARE: Horizontal scale, morphology, and rainfall production. *J. Atmos. Sci.,* **55,** 2715–2729.

Saxen, T. R., and S. A. Rutledge, 1998: Surface fluxes and boundary layer recovery in TOGA COARE: Sensitivity to convective organization. *J. Atmos. Sci.,* **55,** 2763–2781.

Short, D. A., P. A. Kucera, B. S. Ferrier, J. C. Gerlach, S. A. Rutledge, and O. W. Thiele, 1997: Shipboard radar rainfall patterns within the TOGA COARE IFA. *Bull. Amer. Meteor. Soc.,* **78,** 2817–2836.

Simpson, J., R. F. Adler, and G. R. North, 1988: A proposed Tropical Rainfall Measuring Mission (TRMM) satellite. *Bull. Amer. Meteor. Soc.,* **69,** 278–295.

Steiner, M., R. A. Houze Jr., and S. E. Yuter, 1995: Climatological characterization of three-dimensional storm structure from operational radar and rain gauge data. *J. Appl. Meteor.,* **34,** 1978–2007.

Taylor, R. C., 1973: An atlas of Pacific islands rainfall. Hawaii Institute of Geophysics Report HIG-73-9, 7 pp. [Available from Dept. of Meteorology, University of Hawaii at Manoa, 2525 Correa Rd., Honolulu, HI 96822.]

Tokay, A., and D. A. Short, 1996: Evidence from tropical raindrop spectra of the origins of rain from stratiform versus convective clouds. *J. Appl. Meteor.,* **35,** 355–371.

Tomczak, M., 1995: Salinity variability in the surface layer of the tropical western Pacific Ocean. *J. Geophys. Res.,* **100,** 20 499–20 515.

Webster, P. J., and R. Lukas, 1992: TOGA COARE: The Coupled Ocean–Atmosphere Response Experiment. *Bull. Amer. Meteor. Soc.,* **73,** 1377–1417.

Xie, P., and P. A. Arkin, 1996: Analyses of global monthly precipitation using gauge observations, satellite estimates, and numerical model predictions. *J. Climate,* **9,** 840–858.

——, and ——, 1997: Global precipitation: A 17-year monthly analysis based on gauge observations, satellite estimates, and numerical model outputs. *Bull. Amer. Meteor. Soc.,* **78,** 2539–2558.

Young, G. S., S. M. Perugini, and C. W. Fairall, 1995: Convective wakes in the equatorial western Pacific during TOGA. *Mon. Wea. Rev.,* **123,** 110–123.

Zipser, E. J., 1977: Mesoscale and convective-scale downdrafts as distinct components of squall-line structure. *Mon. Wea. Rev.,* **105,** 1568–1589.

——, R. J. Meitin, and M. A. LeMone, 1981: Mesoscale motion fields associated with a slowly moving GATE convective band. *J. Atmos. Sci.,* **38,** 1725–1750.